Anti-Stokes Photoinduced Electrochemiluminescence at a Photocathode

Julie Descamps, Yiran Zhao, Jing Yu, Guobao Xu, Yoan Léger, Gabriel Loget, Neso Sojic

Anti-Stokes Photoinduced Electrochemiluminescence at a Photocathode

Julie Descamps,[a] Yiran Zhao,[b] Jing Yu,[a] Guobao Xu,[c] Yoan Léger,[d] Gabriel Loget,*[b] Neso Sojic *[a,c]

Anti-Stokes photoinduced electrochemiluminescence (PECL) converts infrared photons to visible photons and is usually triggered at a narrow bandgap protected photoanode. Here, we report the first example of PECL with the model $[Ru(bpy)_3]^{2+}$/ benzoyl peroxide system at a bare *p*-type Si photocathode. The reported PECL system, which allows to notably decrease the cathodic potential required for ECL generation should open new opportunities for imaging and light-addressable devices.

Photoinduced electrochemiluminescence (PECL) is a research field that combines absorption and emission photoelectrochemistry, i.e., photoelectrochemistry at illuminated semiconductors (SCs) and electrochemiluminescence (ECL).[1–3] ECL is the emission of light caused by the excited state of a luminophore generated by redox reactions at an electrode surface.[4] Most applications of ECL rely on the use of model ECL luminophores such as tris(bipyridine)ruthenium(II) complex ($[Ru(bpy)_3]^{2+}$), or luminol (3-aminophthalhydrazide), and their analogs.[5–7] ECL has become a powerful analytical method, especially for immunoassays and clinical diagnosis,[8,9] and is promising for bio-imaging.[10–13] On the other hand, in photoelectrochemistry at illuminated SCs, a depleted SC absorbs photons to generate minority charges carriers that participate in redox reactions at the solid/liquid interface.[14–16] PECL couples these two concepts together by employing absorption at a depleted SC to emit ECL, which enables Stokes or anti-Stokes-type photon conversion (depending on the SC bandgap, the excitation wavelength, and the ECL system employed).[3] Anti-Stokes PECL is based on the use of a narrow-bandgap SC as a photoelectrode, which is challenging due to poor stability in operation conditions.[17,18] However, progress made on photoelectrode materials and SC protection strategies recently allowed to promote considerable progress in PECL. For instance, the infrared (IR)-to-visible conversion of photons by anti-Stokes PECL was demonstrated with $[Ru(bpy)_3]^{2+}$/TPrA,[19,20] and the luminol/H_2O_2 systems at *n*-type Si (*n*-Si) based photoanodes.[21] In this approach, Si is particularly prone to anodic corrosion processes and requires the use of protection strategies, i.e., its coverage by an oxide and a metal thin film[19,20] or the covalent grafting of an organic monolayer.[21] An anodic ECL system was also investigated using more stable oxide-based *n*-type SCs photoanodes ($BiVO_4$ or α-Fe_2O_3), but the higher bandgap value of such materials only allowed Stokes-type PECL conversion.[22,23] Nevertheless, several narrow bandgap SCs are relatively stable in the photocathodic regime, which makes their use as photocathodes an important and straightforward alternative for stable anti-Stokes PECL. This strategy has been unexplored since the mid-seventies when anti-Stokes cathodic PECL was proposed with a diphenylanthracene derivative through ion annihilation pathway.[3]

In this communication, we report the cathodic PECL at hydrogenated *p*-type Si (*p*-Si) using a coreactant mechanism where $[Ru(bpy)_3]^{2+}$ acts as a luminophore and benzoyl peroxide (BPO) as a sacrificial coreactant, as depicted in **Figure 1a**. In our experiments, *p*-Si was selected because of its availability, its narrow bandgap, and its stability at cathodic bias.[24–28] Indeed, as opposed to anodic bias, no dramatic degradation is expected for freshly hydrogenated (treated by a 10% HF solution) Si electrodes rapidly immersed in the electrolyte and used under cathodic bias.[24–28] Si has a bandgap of 1.12 eV (**Figure 1b**, blue line), meaning that it can absorb incident photons with a wavelength shorter than 1.1 µm.[29] Therefore, we employed an IR light-emitting diode (LED, λ_{LED} = 850 nm) as an excitation source, as shown in **Figure 1b.** We selected this incident wavelength because it corresponds to a high external quantum yield for Si photocathodes,[28,30] and it is far enough from the ECL emission band. Under illumination, free electrons (e^-) are photogenerated within the Si layer and can diffuse towards the depletion region of the *p*-Si to participate to the electrochemical reaction. At the *p*-Si/electrolyte interface, they reduce BPO to $BPO^{\bullet-}$ and $[Ru(bpy)_3]^{2+}$ to $[Ru(bpy)_3]^{+}$. $BPO^{\bullet-}$ irreversibly decomposes, giving a strongly reactive radical[31,32] that oxidizes $[Ru(bpy)_3]^{+}$ with a highly exergonic electron transfer leading to its excited state $[Ru(bpy)_3]^{2+*}$. On Figure 1a, a stepwise dissociative electron transfer reaction of BPO is represented but some previous reports described also the possibility of concerted dissociative electron-transfer reaction of BPO.[33–36] The luminophore returns then to the ground state by emitting a photon at λ_{ECL} = 630 nm (**Figure 1b**, red line). During our experiments, the ECL spectra are recorded continuously with a spectrometer coupled to an optical fiber, as shown in **Figure 1c** (see ESI for more details).

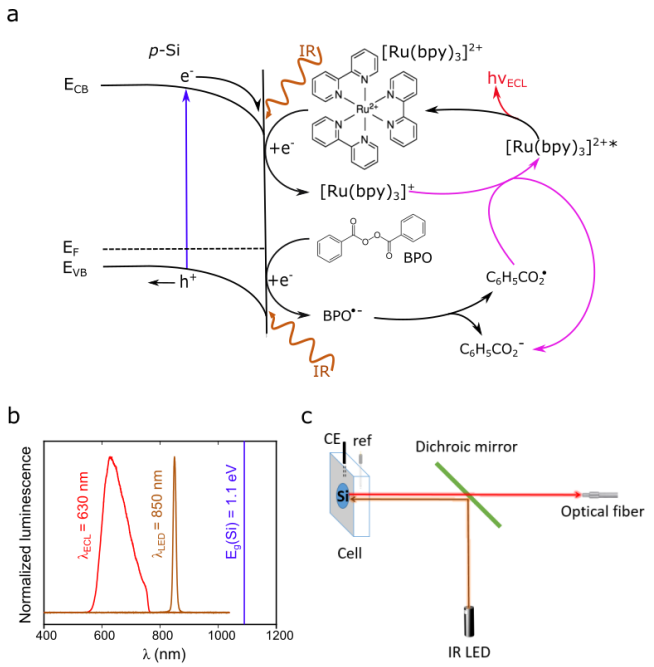

Figure 1. a) Scheme showing the photoinduced charge transfer process and the reaction mechanism occurring at the Si photocathode, initiated by the absorption of IR light (λ_{LED}) and leading to the emission of ECL (λ_{ECL}). **b)** Normalized spectra of: emission of the LED used in this work (brown), PECL emission (red), and bandgap position of *p*-Si (blue). **c)** Scheme of the photoelectrochemical setup employed for the study of PECL.

p-Si was first studied by cyclic voltammetry from 0 to -2 V (all potentials are referred vs. an Ag wire quasi reference electrode) under IR irradiation (6.6 mW cm^{-2}) and in the dark. The cyclic voltammograms (CVs) of **Figure 2a** show that while a relatively low current density is recorded in the dark (dark curve, < -0.69 mA cm^{-2}), a wave with a higher photocurrent density appears from -0.69 V under illumination (red curve). As shown in **Figure 2b**, a strong light emission is detected under illumination from -1.24 V, demonstrating the PECL activity of this photocathode. The ECL spectra recorded during the CVs[37] show an emission band centered at 630 nm typical to the metal-to-ligand charge transfer excited state $[Ru(bpy)_3]^{2+*}$ (**Figure 2c**). In order to compare this PECL behavior with that of ECL, further experiments were performed in the same conditions except that heavily doped non-photoactive n^+-Si electrodes (essentially behaving as a conductor) were studied in the dark (blue curve). The blue curves of **Figures 2a,b** show that, in this case, a strong cathodic wave associated with ECL emission can be observed at much more negative potentials. It is also clearly visible by comparing the ECL spectra collected on both SCs during the CVs (**Figure 2c**). This highlights the effect of the photovoltage generated in the depleted *p*-Si, which shifts the emission onset potential. This is clearly illustrated by the fact that the potential of maximum emission is shifted by a considerable value of +0.51 V for PECL at the *p*-Si photocathode when compared with ECL at the n^+-Si cathode. A comparative study done on a series of 7 *p*-Si photocathodes and 5 n^+-Si cathodes revealed that the onset potential values for emission can vary within a relatively large ≈200 mV potential range. This behavior is attributed to difference in the state of the Si surface, which can be altered during its handling in air between the chemical hydrogenation and the electrochemical study.

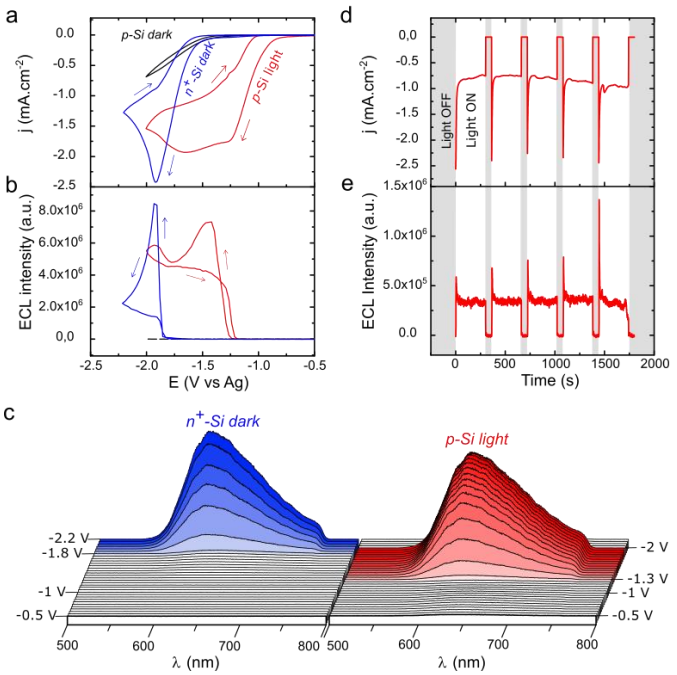

Figure 2. a) CVs recorded under IR illumination on *p*-Si (red) and in the dark on *p*-Si (black) and on n^+-Si (blue). b) Corresponding ECL intensity profiles. Scan rate: 50 mV s^{-1}. c) ECL spectra recorded as a function of potential recorded in the dark on n^+-Si (blue) and under IR illumination on *p*-Si (red). d) Chronoamperogram recorded at -1.6 V at *p*-Si while imposing successive ON/OFF cycles with the LED. e) Corresponding ECL intensity profiles. The measurements were performed in 1 mM $[Ru(bpy)_3]^{2+}$ + 10 mM BPO + 0.2 M $TBAPF_6$ in acetonitrile.

The PECL stability was then studied under potentiostatic control (E_{app} = -1.6 V) by alternatively turning the IR LED (P = 6.6 mW cm^{-2}) on for 5 min and off for 1 min for an overall time of 30 min. We checked the potential heating effect of the LED and the temperature of the electrolyte solution was constant for 30 min. under LED illumination. The chronoamperogram (CA) shows that the photocurrent density (**Figure 2d**) and the PECL signals (**Figure 2e**) are stable for 25 min. and instantly responds to illumination condition. These results show that stable PECL emission can be generated for 25 min. at hydrogenated *p*-Si-based photocathodes. The ECL instability observed after 25 minutes may be related to some side-products generated by the continuous reduction of BPO or to the accumulation of these side-products that may quench the ECL emission.

To conclude, we have reported the first example of cathodic PECL using $[Ru(bpy)_3]^{2+}$ as a luminophore. The emission occurs through a reductive-oxidation pathway with BPO employed as a sacrificial co-reactant. We have shown that hydrogenated *p*-Si can be used for anti-Stokes PECL for converting invisible IR light (λ_{LED} = 850 nm) to visible light (λ_{ECL} = 630 nm) with satisfying stability in operation. This study demonstrates that the use of a photocathode represents a relatively simple and reliable alternative for upconversion PECL when employed

with cathodic ECL systems, which is promising for future development in PECL.

Conflicts of interest

There are no conflicts to declare.

Acknowledgements

This work was funded by ANR (LiCORN, ANR-20-CE29-0006). J. Y. acknowledges the China Scholarship Council for her PhD fellowship. N. S. and G. X. thank the support from the CAS President's International Fellowship Initiative (PIFI).

References

[1] D. Laser, A. J. Bard, *Chem. Phys. Lett.* **1975**, *34*, 605–610.
[2] J. D. Luttmer, A. J. Bard, *J. Electrochem. Soc.* **1979**, *126*, 414–419.
[3] Y. Zhao, L. Bouffier, G. Xu, G. Loget, N. Sojic, *Chem. Sci.* **2022**, *13*, 2528–2550.
[4] N. Sojic, *Analytical Electrogenerated Chemiluminescence: From Fundamentals to Bioassays*, The Royal Society Of Chemistry, **2020**.
[5] Z. Liu, W. Qi, G. Xu, *Chem. Soc. Rev.* **2015**, *44*, 3117–3142.
[6] X. Zhou, D. Zhu, Y. Liao, W. Liu, H. Liu, Z. Ma, D. Xing, *Nat. Protoc.* **2014**, *9*, 1146–1159.
[7] E. Kerr, E. H. Doeven, D. J. D. Wilson, C. F. Hogan, P. S. Francis, *Analyst* **2016**, *141*, 62–69.
[8] H. Qi, C. Zhang, *Anal. Chem.* **2020**, *92*, 524–534.
[9] F. Du, Y. Chen, C. Meng, B. Lou, W. Zhang, G. Xu, *Curr. Opin. Electrochem.* **2021**, *28*, 100725.
[10] G. Valenti, S. Scarabino, B. Goudeau, A. Lesch, M. Jović, E. Villani, M. Sentic, S. Rapino, S. Arbault, F. Paolucci, N. Sojic, *J. Am. Chem. Soc.* **2017**, *139*, 16830–16837.
[11] J. Zhang, S. Arbault, N. Sojic, D. Jiang, *Annu. Rev. Anal. Chem.* **2019**, *12*, 275–295.
[12] C. Ma, Y. Cao, X. Gou, J.-J. Zhu, *Anal. Chem.* **2020**, *92*, 431–454.
[13] J. Dong, Y. Lu, Y. Xu, F. Chen, J. Yang, Y. Chen, J. Feng, *Nature* **2021**, *596*, 244–249.
[14] H. Gerischer, *Electrochim. Acta* **1990**, *35*, 1677–1699.
[15] R. Memming, *Semiconductor Electrochemistry*, Wiley-VCH, Weinheim, **2015**.
[16] M. X. Tan, P. E. Laibinis, S. T. Nguyen, J. M. Kesselman, C. E. Stanton, N. S. Lewis, in *Prog. Inorg. Chem.* (Ed.: K.D. Karlin), Wiley-VCH, Weinheim, **1994**, pp. 21–144.
[17] A. J. Bard, M. S. Wrighton, *J. Electrochem. Soc.* **1977**, *124*, 1706–1710.
[18] D. Bae, B. Seger, P. C. K. Vesborg, O. Hansen, I. Chorkendorff, *Chem. Soc. Rev.* **2017**, *46*, 1933–1954.
[19] Y. Zhao, J. Yu, G. Xu, N. Sojic, G. Loget, *J. Am. Chem. Soc.* **2019**, *141*, 13013–13016.
[20] Y. Zhao, J. Descamps, S. Ababou-Girard, J.-F. Bergamin, L. Santinacci, Y. Léger, N. Sojic, G. Loget, *Angew. Chem. Int. Ed.* **2022**, DOI doi.org/10.1002/ange.202201865.
[21] Y. B. Vogel, N. Darwish, S. Ciampi, *Cell Rep. Phys. Sci.* **2020**, *1*, 100107.
[22] J. Yu, H. Saada, R. Abdallah, G. Loget, N. Sojic, *Angew. Chem. Int. Ed.* **2020**, *59*, 15157–15160.
[23] J. Yu, H. Saada, N. Sojic, G. Loget, *Electrochim. Acta* **2021**, *381*, 138238.
[24] K. Sun, S. Shen, Y. Liang, P. E. Burrows, S. S. Mao, D. Wang, *Chem. Rev.* **2014**, *114*, 8662–8719.
[25] Y. Nakato, H. Yano, S. Nishiura, T. Ueda, H. Tsubomura, *J. Electroanal. Chem. Interfacial Electrochem.* **1987**, *228*, 97–108.
[26] R. N. Dominey, N. S. Lewis, J. A. Bruce, D. C. Bookbinder, M. S. Wrighton, *J. Am. Chem. Soc.* **1982**, *104*, 467–482.
[27] Y. Hou, B. L. Abrams, P. C. K. Vesborg, M. E. Björketun, K. Herbst, L. Bech, A. M. Setti, C. D. Damsgaard, T. Pedersen, O. Hansen, J. Rossmeisl, S. Dahl, J. K. Nørskov, I. Chorkendorff, *Nat. Mater.* **2011**, *10*, 434–438.
[28] J. Tourneur, B. Fabre, G. Loget, A. Vacher, C. Mériadec, S. Ababou-Girard, F. Gouttefangeas, L. Joanny, E. Cadot, M. Haouas, N. Leclerc-Laronze, C. Falaise, E. Guillon, *J. Am. Chem. Soc.* **2019**, *141*, 11954–11962.
[29] Z. Chen, T. G. Deutsch, H. N. Dinh, K. Domen, K. Emery, A. J. Forman, N. Gaillard, R. Garland, C. Heske, T. F. Jaramillo, A. Kleiman-Shwarsctein, E. Miller, K. Takanabe, J. Turner, in *Photoelectrochem. Water Split.* (Eds.: Z. Chen, H.N. Dinh, E. Miller), Springer New York, New York, NY, **2013**, pp. 49–62.
[30] S. W. Boettcher, E. L. Warren, M. C. Putnam, E. A. Santori, D. Turner-evans, M. D. Kelzenberg, M. G. Walter, J. R. Mckone, B. S. Brunschwig, H. A. Atwater, N. S. Lewis, *J. Am. Chem. Soc.* **2011**, 1216–1219.
[31] M. Hesari, Z. Ding, *J. Electrochem. Soc.* **2016**, *163*, H3116–H3131.
[32] F. Polo, F. Rizzo, M. Veiga-Gutierrez, L. De Cola, S. Quici, *J. Am. Chem. Soc.* **2012**, *134*, 15402–15409.
[33] S. Antonello, F. Maran, *J. Am. Chem. Soc.* **1999**, *121*, 9668–9676.
[34] S. Antonello, F. Maran, *J. Am. Chem. Soc.* **1997**, *119*, 12595–12600.
[35] S. Antonello, M. Musumeci, D. D. M. Wayner, F. Maran, *J. Am. Chem. Soc.* **1997**, *119*, 9541–9549.
[36] S. Antonello, M. Hesari, F. Polo, F. Maran, *Nanoscale* **2012**, *4*, 5333–5342.
[37] M. Hesari, Z. Ding, *Nat. Protoc.* **2021**, *16*, 2109–2130.